www.ijarp.com ISSN 2456-9992 Page: 01-14

Research Article

International Journal Advanced Research Publications

Volume: 02

Issue: 11

THERMOELECTRIC AND MECHANICAL PROPERTIES OF TIN SELENIDE AND TIN TELLURIDE CHALCOGENIDES: A FIRST-PRINCIPLES INVESTIGATION

Salihu Ibrahim*[1], Abubakar Yakubu[2], Yahaya Abubakar Aliero[3]

[1]Department of Physics, Faculty of Science, Zamfara state university Talata Mafara, ZAMSUT. Zamfara State, Nigeria.

[2]Department of Physics, Faculty of Physical Science, Abdullahi Fodio University of Science and Technology Aliero, Kebbi State, Nigeria.

[3]Department of Physics, Faculty of Physical Science, Abdullahi Fodio University of Science and Technology Aliero, Kebbi State, Nigeria.

Article Received: 13 October 2026, Article Revised: 02 November 2026, Published on: 21 November 2026

***Corresponding Author: Salihu Ibrahim**

Department of Physics, Faculty of Science, Zamfara state university Talata Mafara, ZAMSUT. Zamfara State, Nigeria.

Doi: https://doi-doi.org/101555/ijrpa.6118

ABSTRACT

The increasing demand for renewable energy technologies necessitates the exploration of efficient materials for energy conversion. Tin chalcogenide compounds such as SnA (A = S, Se, Te) are of significant interest due to their promising physical properties. These materials integrate elements from groups IV (Sn), and VIA (S, Se, Te) of the periodic table, resulting in chemically stable and potentially tunable semiconductors. In particular chalcogenides, are known for their excellent thermoelectric, optical, and electronic behaviors making them strong candidates for use in solar cells, infrared detectors, and solid-state thermoelectric devices. This study presents a comprehensive first-principles investigation of the mechanical, and thermoelectric properties of tin chalcogenides (SnA, where A = Se, Te) using Quantum ESPRESSO code. The calculations were performed using GGA-PBE and GGA-PBESol, exchange-correlation functionals, to ensure strong predictions. The elastic constants confirm that, the compounds are mechanically stable in their cubic phase, satisfying the Born-Huang criteria. Mechanical property analysis, including Pugh's ratio and Cauchy pressure, reveals that SnSe and SnTe are brittle. The study parameters for thermoelectric performance includes, electrical conductivity, Seebeck coefficient, power factor, electronic thermal conductivity, and figure of merit (ZT) calculated over temperature range of ~200–1200 K.

The results show that, SnSe is a superior thermoelectric material, with its power factor and ZT increasing significantly with temperature, exceeding a ZT of 1 at high temperatures (around 1000-1200 K). While SnTe exhibits poor thermoelectric efficiency due to its high electronic thermal conductivity. This research highlights SnSe as a highly promising material for high-temperature thermoelectric applications.

KEYWORDS: Tin Chalcogenides, Density Functional Theory (DFT), First-Priciple Study, Figure of Merit (ZT), Seebeck Coefficient.

1. INTRODUCT ION

There exists a rising need for renewable energy and greater energy efficiencies due to the limited supply of non-renewable energy sources such as fossil fuels. New technological advances are required to achieve the necessary growth, particularly in the areas of photovoltaics (PV) and thermoelectrics (TE) (International Energy Agency, 2023). Beyond silicon, material classes such as sulphide, selenide, telluride, perovskites, oxides, and organic materials have been commonly studied for solar energy conversion ((Javed *et al*., 2020), (Kare *et al*., 2020), (Mitic *et al*., 2024), (Yahaya *et al*., 2023), (Yahaya *et al*., 2024), (Yuel *et al*., 2024), (Zhao *et al*., 2017), (Bafekry *et al*., 2021), (Burton *et al*., 2013), (Burnuiana *et al*., (2025)). Chalcogenide is a chemical compound consist of at least one chalcogen anion and at least one or more electropositive element. All group 16 elements are defined as chalcogens. Tin (Sn) chalcogenides are chemical compounds composed of tin (Sn) and one of the chalcogen elements of group 16 in the periodic table (oxygen (O), sulfur (S), selenium (Se), tellurium (Te) and polonium (Po)). These materials generally follow the formula A-X, where A are metals, (Sn) and X is chalcogen. These compounds integrate tin (Sn), and a chalcogen element sulfur (S), selenium (Se), or tellurium (Te), forming framework or layered structures with potentially tunable band gaps, good thermal stability and favorable charge transport characteristics (Kare *et al*., 2020).

Previously studied material classes for thermoelectric (TE) and Optoelectronic applications include mono layers tin chalcogenides such as SnX (X=Se,S), 2D tin Chalcogenide SnX (X=Te,S), SnTe, tin chalcogenide SnS and SnSe, SnTe-baseb, ternary cacogenides, XIn_2S_4 (X=Zn,Cd,Hg), $AlAuO_2$ and $AlAu_{094}Fe_{006}O_2$, double proveskite Rb_2SeX_6 (X=Cl,Br) ((Batool *et al*., 2022), (Dong *et al*., 2019), (Fatahi *et al*., 2020), (Wang *et al*., 2025), (Rundle & Leon 2022), (Rajabi Alzahrani *et al*., 2025), (Yahaya *et al*., 2024)). Earlier works have also suggested these two compounds (SnSe and SnTe) to be appealing for thermoelectric

applications ((Fatahi *et al*., 2020), (Rundle and Leon 2022)). SnSe, SnTe has been highlighted specifically for its unique electronic band structure, showing regions of the Brillouin zone with both high and low dispersion of strong character. These properties, along with substantial acoustic-optical phonon mixing, suggest SnSe, SnTe to be a promising candidate for application in thermoelectric devices (More *et al*., 2023).

Despite their promising nature, the SnA (A= Se, Te) compounds have not been comprehensively studied, especially through a comprehensive first-principles approach. There is a noticeable gap in the literature concerning the simultaneous investigation of their structural, electronic, optical, mechanical, and thermoelectric properties. This study will fill the gap by using two exchange correlation functions GGA-PBE and GGA-PBESol.

2. COMPUTATIONAL DETAILS

The mechanical and thermoelectric properties of tin chalcogenide (SnA, where A = S, Se, Te) were calculated using the Quantum ESPRESSO code (Giannozzi *et al.,* 2009). A plane-wave basis set was employed to represent electron wavefunctions. Electron-ion interactions was described using norm-conserving pseudopotentials, and the exchange-correlation functionals used was Generalized Gradient Approximation (GGA) in both the Perdew–Burke–Ernzerhof (PBE) and Perdew–Burke–Ernzerhof for solids (PBESol) (Perdew *et al.,* 1992; Perdew *et al.,* 1996).

SnS and SnSe have a space group of Pnma with orthorhombic crystal structure while SnTe have a space group of Fm-3m with a cubic crystal structure. Lattice Parameters for SnS and SnSe are a ≈ 4.33 Å, b ≈ 11.19 Å, c ≈ 3.98 Å and a ≈ 4.15 Å, b ≈ 11.50 Å, c ≈ 4.44 Å respectively. While SnTe have a Lattice Parameters of a ≈ 6.32 Å. The calculations used a kinetic energy cut-off of 100 Ry and a 6 × 6 × 6 k-point mesh for Brillouin zone integration. A plane-wave cut-off of 120 Ry, energy convergence criterion of 10^{-5} eV, and a force convergence threshold of 10^{-5} eV/Å were used during structural optimization.The thermoelectric (TE) properties of the studied tin chalcogenides materials SnA (A = Se, Te) were calculated using plane wave basis set of Quantum ESPRESSO (QE) code using both GGA (PBE and PBESol) exchange–correlation functionals. Electronic thermal conductivity (κ_e), Seebeck coefficient (S), electrical conductivity (σ), power factor (PF), and figure of merit (ZT) are the thermoelectric properties calculated in this study. The plane wave package operates within the framework of DFT, as implemented in the QE code, and a relaxation time constant of (= 10 14 s) was used. Figure of merit (ZT) is strongly influenced by the Seebeck coefficient (S) and electronic thermal conductivity (κ_e), and these thermoelectric parameters

depend on the relaxation time constant. All the TE properties are calculated within temperature (T) values in the range of 150–1300 K. Power factor is calculated using:

$$PF = S^2\sigma \quad (1)$$

While the figure of merit (ZT) was computed using:

$$ZT = \frac{\sigma S^2}{\kappa_e}T \quad (2)$$

The mechanical behavior of a material can be examined from the investigation of the elastic constants Cij. In response to an employed macroscopic stress is explained by criterion of elastic constant parameters. Elastic constants Cij of solids provide the physical connection with the mechanical and active functioning, it defines how a deformations is caused by the stress and then retrieve to restores its original form following the stress ended, Cij are essential parameters of a material in order to give useful information about the structure stability, anisotropic character and the bonding character within adjoining atomic planes. Cubic compounds have three self-reliant elastic constants of the kinds C_{11}, C_{12} and C_{44}. The cubic unit cell is distorted after applying a proper strain tensor resulting in an energy strain relationship to determine these parameters. Verify mechanical stability criteria (Born-Huang conditions).

A crystal cannot exist in a stable or meta-stable state unless its elastic constants satisfy the generalized mechanical stability criteria. The Born–Huang elastic criteria theorem is given as:

$$C_{11} - C_{12} > 0, \quad (3)$$

$$C_{11} - 2C_{12} > 0, \quad (4)$$

$$C_{44} > 0, \quad (5)$$

And

$$C_{11} < B < C_{44} \quad (6)$$

The bulk modulus (B), will be determine using:

$$B = \frac{C_{11} + C_{12}}{2} \quad (7)$$

The following are Voigt's elastic moduli equations

$$B_V = \frac{C_{11} + 2C_{12}}{3}. \quad (8)$$

$$G_V = \frac{C_{11} - C_{12} + 3C_{44}}{5}. \quad (9)$$

Where B_V and G_V are the isotropic bulk modulus and shear modulus, respectively. For a cubic structure, Reuss's bulk modulus (B_R) and Voigt's bulk modulus (B_V) are equivalent. Reuss's shear modulus (G_R) is expressed as follows:

$$G_R = \frac{5(C_{11} - C_{12})C_{44}}{4C_{44} + 3(C_{11} - C_{12})} \quad (10)$$

Ductility & Brittleness Analysis: Use Pugh's ratio (B/G) and Poisson's ratio to classify materials as ductile or brittle. Evaluate hardness using empirical models (e.g., Tian's model). Anisotropy: Compute anisotropic indices (e.g., universal anisotropy index, shear anisotropy factor). Visualize anisotropy using 3D surface plots of elastic moduli (Saba *et al*., 2016).

Poisson's Ratio: The dimensionless relationship between lateral deformation and axial deformation is another constant, named Poisson's ratio, and describes the elastic deformations that a material can undergo in the three spatial directions. Poisson's ratio is an essential metric that reveals properties like brittleness or ductility, shear stability, and the nature of interatomic forces as expressed in equation (11) and (12). Poisson's ratio greater than 0.26 indicates ductility in materials, while values less than 0.26 indicate brittleness.

$$\nu = \varepsilon \quad (11)$$

$$V = \frac{3B - 2G}{6B + 2G} \quad (12)$$

Cauchy pressure (PC) is a mechanical parameter that determines brittleness and ductility of a studied alloy material. Equation (12) was used to calculate PC of the studied alloy materials, if PC is negative the material is said to be brittle material and if it's positive, the material is said to be solid materials,

$$Y = \frac{9BG}{3B + G} \quad (13)$$

Isotropy, in the context of material properties, refers to the condition where a material exhibits the same properties in all directions. An isotropic material is one that has properties considered to be independent of the direction one picks to examine the material.

In optically isotropic materials, it is $\varepsilon_1 = \varepsilon_2 = \varepsilon_3$ which means that the optical properties are non-directional. An isotropy can be determine using:

$$A = \frac{2C_{44}}{C_{11} - C_{12}} \quad (14)$$

Young modulus is a mechanical property of solid that measures the tensile or compressive stiffness when force is applied length wise. It's the ratio of the stress (force per unit area) applied to the object and the resulting axial strain (deformation) in the linear elastic region of the material.

$$E = \frac{\sigma}{\varepsilon} \tag{15}$$

The Hill's elastic moduli approximation is used to get the average of Voigt's and Reuss' elastic moduli values

$$B_H = \frac{1}{2}(B_V + B_R) \tag{16}$$

$$G_H = \frac{1}{2}(G_V + G_R) \tag{17}$$

Pugh's ratio (R_P) is the ratio of B to G. Frantsevich's ratio (R_F) is the ratio of shear modulus to the bulk modulus and is also known as the inverse of Pugh's ratio. Pugh's ratio and Frantsevich's ratio can be determined using equation (18) and (19).

$$R_P = \frac{B}{G} \tag{18}$$

$$R_F = \frac{G}{B} \tag{19}$$

2. RESULTS AND DISCUSSION

3.1 Thermoelectric Properties

Materials with good thermoelectric properties can be used to convert thermal energy (heat) to electrical energy (Kare *et al*., 2020). The movement of charges for energy transfer produces a heat gradient, which results in a potential difference and a thermoelectric effect. Thermoelectric refrigerators, detectors, and cooling systems are some of the practical applications of thermoelectric materials (More *et al*., 2023).

3.1.1 Electrical conductivity

Electrical conductivity (σ) plots for tin chalchogenides materials SnA (A = Se and Te) versus a temperature range of 200-1200 K are described in Figure 1 (a) and (b).

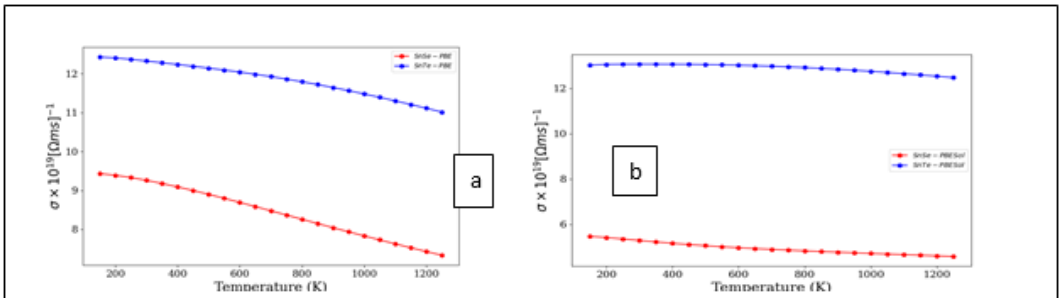

Figure 1 Electrical Conductivity of SnSe and SnTe usind (a) PBE (b) PBESol.

For both SnSe and SnTe, using both PBE and PBESol functionals, the electrical conductivity (σ) decreases with increase in temperature (from ~200 to 1200 K), demonstrating metallic behavior, where increased lattice vibrations at higher temperatures scatter charge carriers more effectively, and reducing conductivity.

3.1.2 Power Factor

The power factor (PF) is a crucial factor to consider when determining a material's suitability for thermoelectric applications. It is defined as the product of Seebeck coefficient and electrical conductivity, equation (1) (Yahaya, *et al*., 2023). Figure 2 (a) and (b) show PF plots against temperature (200–1200 K range).

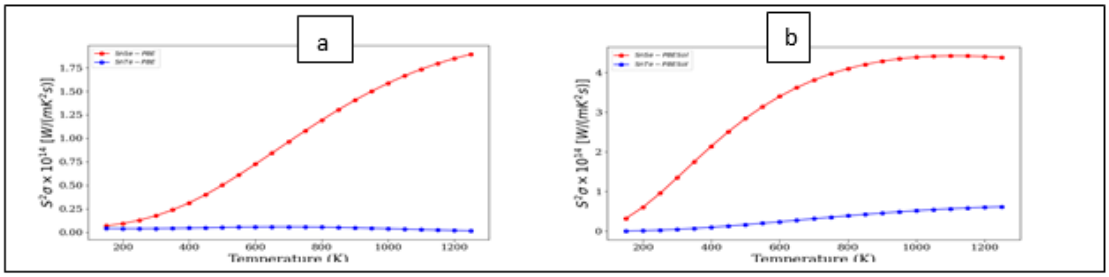

Figure 2 Power Factor of SnSe and SnTe usind (a) PBE (b) PBESol.

Figure 2 (a) and (b) shows that, SnSe reaches a high power factor due to its exceptionally large Seebeck coefficient. The PF of SnSe increases with increase in temperature, becoming the superior material at high temperatures (~ 600-800 K), while that of SnTe is at low value ~4 x 10^{11} W/m.K^2.s, benefiting from its very high electrical conductivity. However, its power factor increases more slowly with temperature compared to SnSe because its Seebeck coefficient is lower.

3.1.3 Seebeck Coefficient

Seebeck coeffcient (S), also known as thermopower, is another important parameter related to material electronic structure. It is defined as the magnitude of an induced thermo electric voltage caused by a temperature gradient within the material (Yahaya, *et al*., 2023). Depending on the material, thermopower can be positive or negative. The dominant hole charge carrier is rep resented by positive Seebeck coefficients, while the dominant electron charge carrier is represented by negative Seebeck coefficients. The plots of calculated Seebeck coefficients of the studied tin chalcogenide materials are shown in Figure 3 (a) and (b).

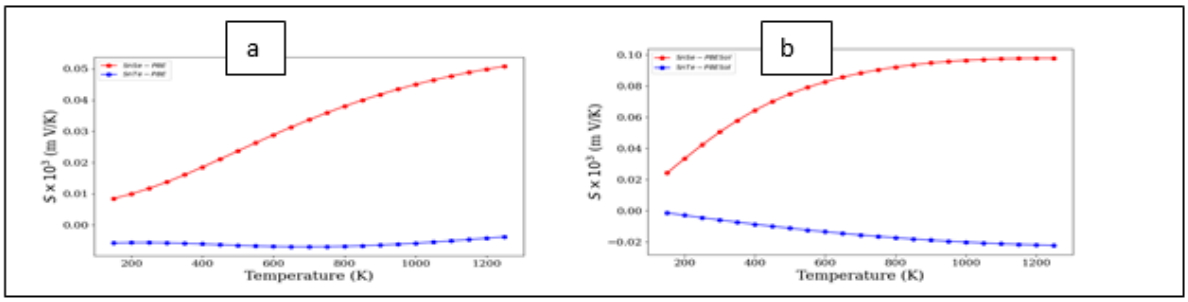

Figure 3 Seebeck Coefficient of SnSe and SnTe usind (a) PBE (b) PBESol.

Figure 3 (a) and (b) described the positive Seebeck coefficient for both SnSe and SnTe ranging from ~200-1200 K, confirming p-type conduction. The coefficient increases with increase in temperature for both materials, but SnSe demonstrates a substantially higher value, rising to ~275 μV/K (PBE) and 300 μV/K (PBESol) at ~1200 K, while SnTe plateaus at a much lower value of around 50-60 μV/K. This establishes SnSe as the superior material for generating a high thermoelectric voltage due to its more favorable electronic structure.

3.1.4 Thermal Conductivity

Thermal conductivity is another thermo-electric property parameter that combines the effect of electronic (κ_e) and lattice thermal conductivity (l). Only the electronic contribution of thermal conductivity is calculated by the BoltzTrap2 code (Madsen, *et al*., 2018). A good thermo-electric material has a low carrier resistance, which results from lower thermal conductivity, resulting in less carrier collision and heating (Hassan, *et al*., 2017). Electronic thermal conductivity calculated for SnSA (A = Se, Te) using GGA-PBE and GGA-PBESol are shown in Figure 4 (a) and (b).

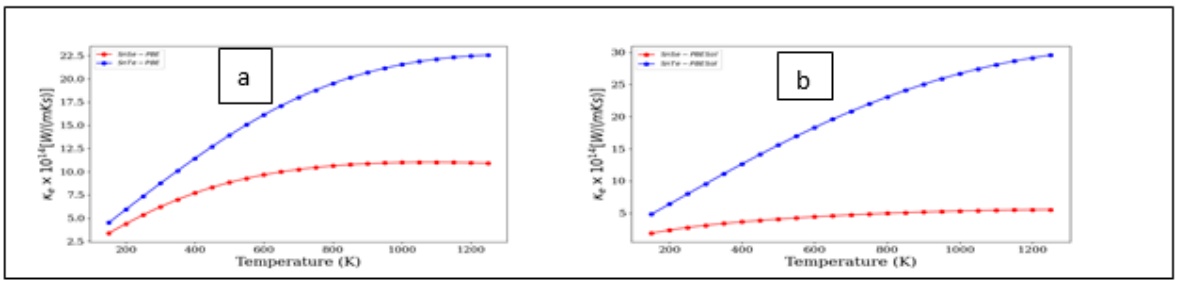

Figure 4 Thermal Conductivity of SnSe and SnTe usind (a) PBE (b) PBESol.

The electronic thermal conductivity (κ_e) for both materials increases with increase in temperature. It's directly linked to the flow of charge carriers (electrical conductivity) via the Wiedemann-Franz law. SnTe has a significantly higher electronic thermal conductivity than SnSe, consistent with its much higher electrical conductivity: For SnTe κ_e rises to ~1.5 W/m.K (PBE) and ~2.5 W/m.K (PBESol). While for SnSe κ_e remains below ~0.5 W/m.K across both functionals. PBESol functional predicts a higher κ_e for both materials compared to the PBE results, which aligns with PBESol also predicting higher electrical conductivity.

3.1.5 Figure of Merit (ZT)

The figure of merit (ZT) demonstrates the higher quality of thermal compounds. Low heat conductivity and electrical properties are the two most essential parameters for assessing increased thermoelectric efficiency. Materials with ZT ≥ 1 are effective thermoelectric materials and are suitable for device engineering (Yahaya, *et al*., 2023).

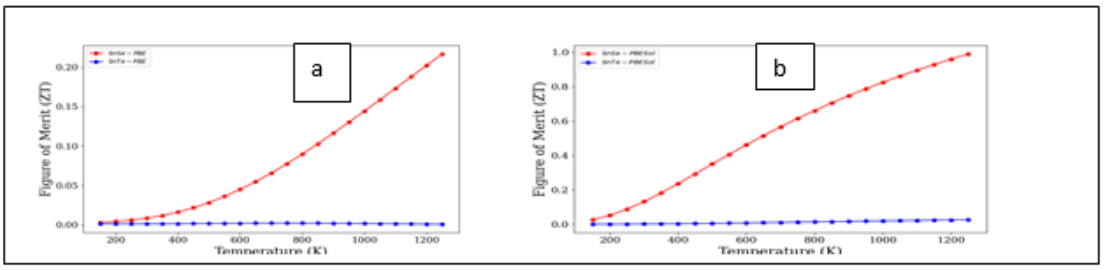

Figure 5 Figure of Merit (ZT) of SnSe and SnTe using (a) PBE (b) PBESol

The ZT plots of SnSe shows a strong and consistent increase with temperature under both functionals. It exceeds ZT=1 at high temperatures (around 1000-1200 K), confirming its excellent potential for high-temperature thermoelectric energy conversion which ZT of SnTe remains low across the entire temperature range. This is primarily a consequence of its very high electronic thermal conductivity (κ_e), which dominates the denominator of the ZT equation and significantly reduces the overall efficiency, despite its favorable power factor at lower temperatures. The plots described that SnSe is a high-performance thermoelectric

material at high temperatures, with ZT > 1, whereas SnTe is inefficient for thermoelectric applications due to its high thermal conductivity. The used of PBESol over PBE leads to a quantitatively higher predicted ZT for SnSe.

3.2 Mechanical Properties

Investigating the mechanical properties of materials play a fundamental role in understanding both their structural stability and binding characteristics (Voigt, 1928). For the cubic systems, only three independent elastic constants (C_{11}, C_{12}, and C_{44}) are required to explain mechanical stability, as presented in Table 1. Particularly, all positive values of elastic constants obey the generalized mechanical stability criteria proposed by Born and Huang, as expressed in equations (3)–(6) (Saba *et al*., 2016), which highlights the stability of SnA (A = Se,Te) tin chalcogenides compounds studied using both GGA-PBE and PBESol in its cubic structure. Employing the Voigt–Reuss–Hill approximations, as outlined in (8) and (9), values of key elastic moduli, including the bulk modulus (B), Young's modulus (Y), and shear modulus (G) for SnA (A = Se,Te) tin chalcogenides compounds using both GGA-PBE and PBESol were computed, as presented in Table 1. A greater shear modulus value shows a material's ductility and resistance to plastic deformation equations (9) and (10). Young's modulus (Y) is a vital mechanical parameter that reflects a material's stiffness; it is defined as the ratio of tensile stress to tensile strain (2.31). A higher value of Young's modulus indicates increased stiffness. Young's modulus (Y) was calculated using equation (15). The results show that, the young modulus for SnSe with GGA-PBE is 73.5585, GGA- PBESol is 7.0586. Cauchy's pressure (P_C), Pugh's ratio (R_P), can be used to determine the material's brittleness or ductility. If the material's Cauchy pressure is negative, it is brittle; otherwise, it is ductile. The studied tin chalcogenides compound SnSe has P_C values for GGA-PBE and GGA-PBESol is (-4.3583) and (75.5905) which show that, the compound are brittle using GGA-PBE and for GGA-PBESol are ductile their P_C values are positive, also the SnTe compound using both GGA-PBE and PBESol are ductile because there P_C values are positive (98.4668) and (119.4606) respectively. Pugh's ratio (R_P) is the ratio of B to G. The values of Pugh's ratio show that SnSe (GGA-PBE and PBESol), and SnTe (GGA-PBE and PBESol), is brittle because its R_P is less than 1.75, as confirmed in table 4.2.

Frantsevich's ratio (R_F) is the ratio of shear modulus to bulk modulus and is also known as the inverse of Pugh's ratio. Compound is said to be brittle if $R_F > 0.571$, otherwise it's a ductile. Frantsevich's ratio of the studied Sn-based chalcogenides compound with $R_F > 0.571$,

such as SnSe (GGA-PBE and PBESol) and SnTe (GGA-PBE and PBESol), are britle as shown in table 1.

Table 1 Calculated values of mechanical properties using GGA-PBE and PBESol for tin chalcogenides SnA (A = Se, Te) compound.

CMPND	EXGGA	C_{11}(GPa	C_{12}(GPa	C_{44}(GPa	B	E	G	ν	R_P	A	R_F	P_C	Y
SnSe	PBE	13.015	11.401	17.373	50.983	73.271	29.201	0.255	0.573	21.537	0.573	-4.358	73.559
	PBESol	94.164	2.610	18.573	33.128	63.433	26.911	0.179	0.8123	O.406	0.812	75.591	7.059
SnTe	PBE	113.634	3.892	15.167	40.472	64.319	26.197	0.228	0.647	0.276	98.467	0.647	64.643
	PBESol	134.894	4.218	15.434	47.777	71.438	28.809	0.240	0.603	0.236	119.461	0.602	71.963

Table 1 lists the computed elastic constants (C_{11}, C_{12}, and C_{44}) for the cubic phases and derived moduli (B, G, E), Poisson's ratio (ν), Pugh's ratio (B/G), Cauchy pressure (P_C), and anisotropy factors (Y). All compounds satisfy the Born–Huang stability criteria, confirming mechanical stability. Bulk and shear moduli decrease from SnSe → SnTe. Pugh's ratio (B/G) < 1.75 and Poisson's ratio (ν) of SnSe and SnTe for both GGA-PBE and PBESol is < 0.26 which indicate that, the compounds are britle. Anisotropy indices show moderate elastic anisotropy, typical of layered chalcogenides.

CONCLUSION

This computational study provides a detailed and theoretical analysis of the mechanical and thermoelectric properties of tin chalcogenides compound SnSe, and SnTe. The investigation confirms the mechanical stability of the compounds. The assessment of ductility and brittleness through Cauchy's pressure and Pugh's ratio classifies SnSe and SnTe as brittle compounds.

The thermoelectric analysis reveals a clear distinction between the materials. SnSe emerges as the most promising material for thermoelectric energy conversion. Its combination of a high Seebeck coefficient and low electronic thermal conductivity allows its figure of merit (ZT) to exceed 1 at higher temperatures, the key benchmark for practical device application. Conversely, SnTe, despite its high electrical conductivity, is rendered inefficient for thermoelectric purposes due to its high electronic thermal conductivity, which strictly limits its ZT. The use of the PBESol functional generally predicts quantitatively higher values for properties like ZT compared to PBE, but does not alter the fundamental trends and material rankings. Therefore, this research successfully identifies SnSe as a high-performance thermoelectric material suitable for further experimental investigation and potential use in high-temperature energy harvesting devices.

REFERENCES

1. Bafekry, A., Shahrokhi, M., Shafique, A., Jappor, H. R., Fadlallah, M. M., Stampfl, C., Ghergherehchi, M., Mushtaq, M., Feghhi, S. A. H., & Gogova, D. (2021). *Semiconducting chalcogenide alloys based on the (Ge, Sn, Pb) (S, Se, Te) formula with outstanding properties: A first-principles calculation study*. ACS Omega, 6(14), 9433–9441. https://doi.org/10.1021/acsomega.0c06024
2. Batool, A., Zhu, Y., Ma, X., Saleem, M. I., & Cao, C. (2022). *DFT study of the structural, electronic, and optical properties of bulk, bilayer Sn-monochalcogenides. Advanced Powder Science Advances,* 3, 100275. https://doi.org/10.1016/j.apsadv.2022.100275
3. Burton, L. A., Colombara, D., Abellon, R. D., Grozema, F. C., Peter, L. M., Savenije, T. J., Dennler, G., & Walsh, A. (2013). *Synthesis, characterization, and electronic structure of single-crystal SnS, Sn_2S_3, and SnS_2. Chemistry of Materials,* 25(24), 4908–4916. https://doi.org/10.1021/cm403046m
4. Buruiana, A.-T., Mihai, C., Kuncser, V., & Velea, A. (2025). *Advances in 2D Group IV monochalcogenides: Synthesis, properties, and applications. Materials*, 18(7), 1530. https://doi.org/10.3390/ma18071530
5. Dong, B., Wang, Z., Hung, N. T., Oganov, A. R., Yang, T., Saito, R., & Zhang, Z. (2019). *New two-dimensional phase of tin chalcogenides: Candidates for high-performance thermoelectric materials. Physical Review Materials,* 3(1), 013405. https://doi.org/10.1103/PhysRevMaterials.3.013405
6. Fatahi, N., Hoat, D. M., Laref, A., Amirian, S., Reshak, A. H., & Naseri, M. (2020*). 2D hexagonal SnTe monolayer: A quasi direct band gap semiconductor with strain sensitive electronic and optical properties. The European Physical Journal B, 93*(32). https://doi.org/10.1140/epjb/e2020-10039-2
7. Giannozzi, P. Andreussi, O. Brumme, T. *et al*., J. *Phys. Condens. Matter* 29, 465901(2017).
8. Hassan, M. I. Arshad, Q. M. "Computational study of electronic, optical and thermoelectric properties of X3PbO(X Ca,Sr,Ba) anti-perovskites", SemicondTechnol. 32 (2017) 115002.
9. International Energy Agency. (2023). *World Energy Outlook 2023. IEA publications. https://www.*
10. *Iea.org/world-energy-outlook-2023*

11. Javed Y., Sikanda M., Mirza, and Rafiz M.A. (2021). *Effect of pressure on mechanical and thermal properties of $SnSe_2$. International journal of thermophysics*, 42,146. https://doi.org/10.1007/s10765-0202894-X
12. Khare, I. S., Szymanski, N. J., Gall, D., & Irving, R. E. (2020). *Electronic, optical and thermoelectric properties of sodium pnictogen chalcogenides: A first principles study. Manuscript submitted for publication. Elsevier.*
13. Madsen, G. K. J. Carrete, & M. J. Verstraete, "BoltzTraP2: A program for interpolating band structures and calculating semi-classical transport coe cients", Comput. Phys. Commun. 231 (2018) 140.
14. Mitić, Ž. Kocić, G., Cvetković, T., & Stankov, M. (2024). *Impact of silicon and quartz on the physiology of maize plants. Clay Minerals,* 59(2), 217–225. doi.org/10.15251/CL.2024.217
15. More, M. P., Patil, S. S., & Tayade, R. J. (2023). First-principles investigation of the structural, electronic, optical, thermoelectric properties of Rb2SeTe6 double perovskite material. Materials Science: Materials in Electronics, 34, 164.doi.org/10.1007/s10854-023-11147-z
16. Rajabi, K., Tashakori, H., Pakizeh, E., & Taghizadeh-Farahmand, F. (2025). *First-principles calculations to investigate electronic, optical and thermoelectrical performances of Pb/Te-based nanolayer & bulk chalcogenides. Inter. Journal of Nano Dimension*, 16(1), 1–?
17. Rundle, J., & Leoni, S. (2022). *Layered tin chalcogenides SnS and SnSe: Lattice thermal conductivity benchmarks and thermoelectric figure of merit. The Journal of Physical Chemistry C,* 126(33), 14036–14046. https://doi.org/10.1021/acs.jpcc.2c02401
18. Saba, N., Jawaid, M., Alothman, O. Y., & Paridah, M. T. (2016). *A review on dynamic mechanical properties of natural fibre reinforced polymer composites. Construction and Building Materials, 106, 149–159.* https://doi.org/10.1016/j.conbuildmat.2015.12.158
19. Wang, L., Moshwan, R., Yuan, N., Chen, Z.-G., & Shi, X.-L. (2025). *Advances and challenges in SnTe-based thermoelectrics. Advanced Materials*, 37(5), 2418280. https://doi.org/10.1002/adma.202418280
20. Yahaya, A. A., Yahya, W. A., & Rahmon, I. A. (2024). *Effect of hydrostatic pressure on opto-electronic, elastic and thermoelectric properties of the double perovskites Rb_2SeX_6 (X = Cl, Br): A DFT study. Applied Sciences and Research*, 3(1), Article 171. https://doi.org/10.46481/asr.2024.3.1.171

21. Yahaya, A. A., Yahya, W. A., Ahmed, A. S., & Sholagberu, A. A. (2024). *Ab initio study of the physical properties of Cs-based double perovskites Cs_2AX_6 (A = Ge, Mn; X = Cl, I). Acta Physica Polonica A,* 145(2), 194–202. https://doi.org/10.12693/APhysPolA.145.194
22. Yahya, W. A., Yahaya, A. A., Adewale, A. A., Sholagberu, A. A., & Olasunkanmi, N. K. (2023). *A DFT study of optoelectronic, elastic and thermo-electric properties of the double perovskites Rb_2SeX_6 (X = Br, Cl). Journal of the Nigerian Society of Physical Sciences,* 5(2), Article 1418. https://doi.org/10.46481/jnsps.2023.1418
23. Yue, J., Zheng, J., Li, J., Shen, X., Ren, W., Liu, Y., & Cui, T. (2024). *Characterization of thermoelectric performance in copper-based chalcogenide $CsCu_3S_2$: Unveiling the role of anharmonic lattice dynamics. arXiv.*doi.org/10.48550/arXiv.2405.04832
24. Zhao, G., Zhang, X., Zhang, Y., Sun, X., & Wang, C. (2017). *First-principles study on the structural, electronic and optical properties of Rb_2SeBr_6 under pressure. Journal of Alloys and Compounds,* 728, 1036–1043. https://doi.org/10.1016/j.jallcom.2017.08.110